








# Preclinical evaluation of a new synthetic carbonate apatite bone substitute on periodontal regeneration in intrabony defects

Jean-Claude Imber<sup>1,2</sup>  | Larissa Carmela Imber<sup>1,2</sup> | Andrea Rocuzzo<sup>1</sup>  |  
Alexandra Stähli<sup>1</sup>  | Fernando Muñoz<sup>3</sup>  | Jens Weusmann<sup>4</sup>  |  
Dieter Daniel Bosshardt<sup>1,2</sup>  | Anton Sculean<sup>1</sup> 

<sup>1</sup>Department of Periodontology, School of Dental Medicine, University of Bern, Bern, Switzerland

<sup>2</sup>Robert K. Schenk Laboratory of Oral Histology, School of Dental Medicine, University of Bern, Bern, Switzerland

<sup>3</sup>Department of Veterinary Clinical Sciences, University of Santiago de Compostela, Ibonelab SL, Lugo, Spain

<sup>4</sup>Department of Periodontology and Operative Dentistry, University Medical Centre of the Johannes Gutenberg University, Mainz, Germany

## Correspondence

Jean-Claude Imber, Department of Periodontology, School of Dental Medicine, University of Bern, Freiburgstrasse 7, CH-3010 Bern, Switzerland.  
Email: [jean-claude.imber@unibe.ch](mailto:jean-claude.imber@unibe.ch)

## Funding information

GC Europe; GC Corporation

## Abstract

**Objective:** To evaluate the potential of a novel synthetic carbonate apatite bone substitute (CO<sub>3</sub>Ap-BS) on periodontal regeneration.

**Background:** The use of various synthetic bone substitutes as a monotherapy for periodontal regeneration mainly results in a reparative healing pattern. Since xenografts or allografts are not always accepted by patients for various reasons, a synthetic alternative would be desirable.

**Methods:** Acute-type 3-wall intrabony defects were surgically created in 4 female beagle dogs. Defects were randomly allocated and filled with CO<sub>3</sub>Ap-BS (test) and deproteinized bovine bone mineral (DBBM) or left empty (control). After 8 weeks, the retrieved specimens were scanned by micro-CT, and the percentages of new bone, bone substitute, and soft tissues were evaluated. Thereafter, the tissues were histologically and histometrically analyzed.

**Results:** Healing was uneventful in all animals, and defects were present without any signs of adverse events. Formation of periodontal ligament and cementum occurred to varying extent in all groups without statistically significant differences between the groups. Residues of both bone substitutes were still present and showed integration into new bone. Histometry and micro-CT revealed that the total mineralized area or volume was higher with the use of CO<sub>3</sub>Ap-BS compared to control ( $66.06 \pm 9.34\%$ ,  $36.11 \pm 6.40\%$ ;  $p = .014$ , or  $69.74 \pm 2.95\%$ ,  $42.68 \pm 8.68\%$ ;  $p = .014$ ). The percentage of bone substitute surface covered by new bone was higher for CO<sub>3</sub>Ap-BS ( $47.22 \pm 3.96\%$ ) than for DBBM ( $16.69 \pm 5.66$ ,  $p = .114$ ).

**Conclusions:** CO<sub>3</sub>Ap-BS and DBBM demonstrated similar effects on periodontal regeneration. However, away from the root surface, more new bone, total mineralized area/volume, and higher osteoconductivity were observed for the CO<sub>3</sub>Ap-BS group compared to the DBBM group. These findings point to the potential of CO<sub>3</sub>Ap-BS for periodontal and bone regeneration.

This is an open access article under the terms of the [Creative Commons Attribution](https://creativecommons.org/licenses/by/4.0/) License, which permits use, distribution and reproduction in any medium, provided the original work is properly cited.

© 2023 The Authors. *Journal of Periodontal Research* published by John Wiley & Sons Ltd.

## KEYWORDS

biomaterial, bone regeneration, histology, intrabony defect, micro-CT, periodontal regeneration

## 1 | INTRODUCTION

Periodontitis is a chronic inflammatory disease caused by dental microbial biofilm resulting in destruction of tooth's supporting tissues leading eventually to tooth loss.<sup>1-3</sup> In periodontitis patients, step I and step II periodontal therapy may not be successful in pocket depth reduction around teeth with initially very deep probing depths or local anatomical peculiarities (e.g., furcation and intrabony defects).<sup>4</sup> Since teeth with enhanced probing depths are at a higher risk for tooth loss,<sup>5</sup> additional therapy is required in the third step of periodontal therapy.<sup>4</sup> For intrabony defects, a surgical approach is still considered the treatment of choice.<sup>6</sup> In intrabony defects, regenerative surgery is usually the treatment of choice due to its increased predictability in restoring the supporting periodontal tissues, which leads to improved clinical and esthetic outcomes compared to conventional periodontal surgery.<sup>7,8</sup> Over the last four decades, various surgical techniques in conjunction with bone substitutes, root surface modification, enamel matrix derivative (EMD), and guided tissue regeneration (GTR) have been employed.<sup>7,9</sup>

Bone substitutes are mainly used in periodontal regenerative procedures to fill the defect, stabilize the blood clot, and maintain the space in order to avoid flap collapse in wide or non-contained intrabony defects.<sup>9</sup> Human histological studies have shown periodontal regeneration (i.e., formation of new cementum, periodontal ligament (PDL), and bone) with the use of autologous bone,<sup>10,11</sup> allogeneic bone,<sup>12,13</sup> xenogeneic bone,<sup>14,15</sup> barrier membranes alone,<sup>16,17</sup> EMD,<sup>18,19</sup> and combinations thereof.<sup>9</sup> In contrast, the use of alloplastic bone substitutes as a monotherapy has failed to yield substantial periodontal regeneration as observed in human histological studies. Periodontal healing following defect fill with synthetic bone substitutes was mainly characterized by a reparative healing characterized by a long junctional epithelium, while periodontal regeneration was either limited to the apical part of the defects or completely absent.<sup>20-23</sup> Bone formation around the graft particles was only occasionally reported, with the particles being mainly encapsulated in soft connective tissue.

Patients' demands and expectations are playing a pivotal role in regenerative periodontal and bone surgery. Since the risk of disease transmission cannot be completely excluded when xenogeneic bone substitutes are used and xenografts are not always accepted by patients for various reasons (e.g., vegetarianism, veganism, and religious issues), a synthetic alternative leading to predictable outcomes would be desirable. Despite its excellent biologic properties, autologous bone has certain disadvantages due to the increase in morbidity caused by the second surgical site and obvious limitations in the donor areas, which may limit harvesting of larger amounts.<sup>24,25</sup>

Synthetic biomaterials made of hydroxyapatite or  $\beta$ -tricalcium phosphate are frequently used in the dental field. Hydroxyapatite

is well known for its stability, whereas  $\beta$ -tricalcium phosphate has a rather fast resorption rate.<sup>26,27</sup> Very recently, a novel synthetic carbonate apatite bone substitute has been introduced to the dental market.<sup>28-32</sup> Preclinical data suggested that the carbonate apatite is only resorbed by osteoclasts, whereas hydroxyapatite is just very minimally resorbed and  $\beta$ -tricalcium phosphate is fast resorbed even in the absence of osteoclasts.<sup>33</sup> Moreover, several preclinical studies have demonstrated excellent biocompatibility and osteoconductive properties of this novel carbonate apatite bone substitute,<sup>28,32,34,35</sup> while clinical studies have also provided evidence for its safety and good clinical outcomes in bone augmentation procedures.<sup>30,31</sup> A very recent clinical study yielded promising results following treatment of deep intrabony defects with the novel synthetic carbonate apatite bone substitute combined with fibroblast growth factor (FGF-2), thus pointing to the clinical relevance of this approach.<sup>29</sup> Nevertheless, according to the best of our knowledge, no data are yet available on the potential effect of this novel synthetic bone substitute on periodontal regeneration. Therefore, the aim of the present study was to evaluate the potential of this novel synthetic biomaterial to promote periodontal regeneration in intrabony defects.

## 2 | MATERIALS AND METHODS

### 2.1 | Animals

Four female, approximately 24 months old, beagle dogs, each weighing 12–15 kg, were used. The animals had an intact dentition and a healthy periodontal status. The animals were kept at the animal facility of the Rof Codina Foundation (Cebiovet, Lugo, Spain). The dogs were housed under laboratory conditions, at a room temperature of 15–21°C and humidity >30 percentage (%). They had access to tap water ad libitum and granulated diet. During the entire study period, the animals were checked once a day for normal behavior, food and water intake, depositions, and presence of pain or illness. Additionally, the weight of each animal was monitored.

The current study was conducted in accordance with the European Communities Council Directive 2010/63/EU and was approved by the Ethics Committee of the Rof Codina Foundation, Lugo, Spain (01/20/LU-001). In addition, the Guidelines for Animal Research: Reporting of In Vivo Experiments (ARRIVE) were included.

### 2.2 | Study design and sample size

The study was designed as a randomized controlled experiment with one test group and two control groups with a randomized assignment to the groups.

Test group: Open flap debridement (OFD) + synthetic carbonate apatite bone substitute (CO<sub>3</sub>Ap-BS, Cytrans® Granules, particle size 0.3–0.6 mm, GC Corporation, Japan)

Positive control group: OFD + deproteinized bovine bone mineral (DBBM, Geistlich Bio-Oss®, particle size 0.25–1.0 mm, Geistlich Pharma, Switzerland)

Negative control group: OFD (alone)

With four animals available and eight sites per animal, a total of 32 sites were treated.

To reduce the risk of bias, the following persons were masked to the experimental allocation: the animal caregivers, the veterinarian responsible for regular check of animals, and the histologist.

### 2.3 | Surgical procedure

The surgical procedure is adapted from a previous study.<sup>36</sup> Briefly, for both surgeries (i.e., tooth extraction and periodontal reconstructive surgery), the animals were sedated with a combination of medetomidine (10 µg/kg/IM, Domitor®, Orion Pharma, Espoo, Finland), morphine (0.4 mg/kg/IM, Morfina Braun 2%, B Braun Medical, Barcelona, Spain), and meloxicam (0.2 mg/kg/IM, Metacam®, Boehringer, Ingelheim am Rhein, Germany) and subsequently anesthetized with propofol (2 mg/kg/IV, Propovet™, Abbott Laboratories, Kent, UK) maintained by inhalation of an O<sub>2</sub> and 2.5%–4% isoflurane mixture (Isobavet®, Schering-Plough, Madrid, Spain). Local anesthesia (Anesvet®, Ovejero, Leon, Spain) was used to reduce perioperative pain and bleeding.

In the first surgery, the first and fourth premolars in the maxilla and the second and fourth premolars in the mandible were extracted bilaterally. The sites were allowed to heal for 12 weeks.

In the second phase, the surgeries were performed by one experienced periodontist (J.-C.I.). Mucoperiosteal flaps were raised, and a coronal reference notch was placed into the tooth at the alveolar crest with a round bur (diameter 0.5 mm). Acute “box-type” 3-wall intrabony defects with dimensions of 4 mm in width (bucco-lingual), 4 mm in depth (apico-coronal), and 7 mm in length (mesio-distal) were surgically created (Figure 1A) by means of rotating and hand instruments. The defects were created mesial to the second premolars and distal to the third premolars in the maxilla. In the mandible, defect creation was performed mesial to the third premolars and mesial to the first molars. Subsequently, the roots were thoroughly scaled to remove the root cementum and PDL. At the apical end of the defect, a second reference notch was created. The notches served as reference points for the histometric measurements. Clinical measurements including the defect depth and width along with intraoral photographs were taken at baseline. The treatment was performed according to the allocated group procedure. In the test group, CO<sub>3</sub>Ap-BS was inserted into the defects (Figure 1B). In the positive control group, the defects were filled with DBBM, whereas the defects were left empty in the negative control group. Thereafter, the flaps were closed (Figure 1C) by means of

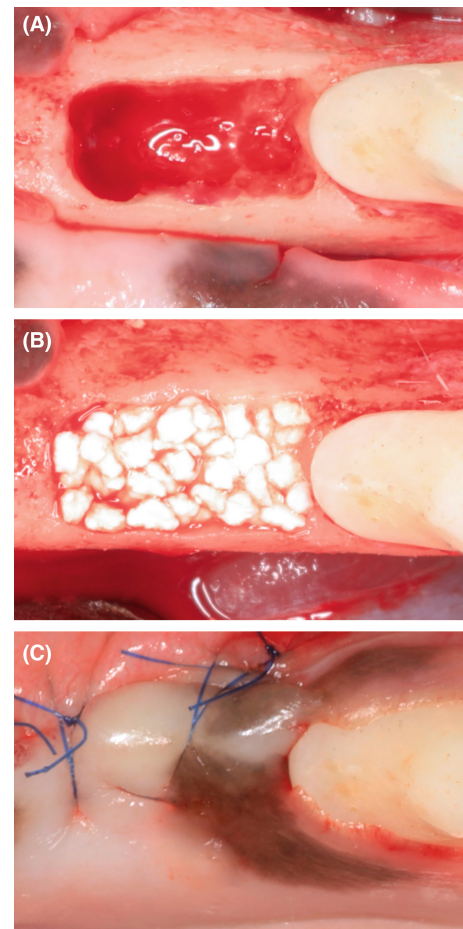


**FIGURE 1** Surgical pictures illustrating the procedure in the test group: (A) after flap elevation and defect creation, (B) application of the biomaterial, and (C) after wound closure.

monofilament sutures (Stoma®-medilene 6-0 blue, Storz am Mark GmbH, Emmingen-Liptingen, Germany).

After the surgeries, the animals received analgesics (meloxicam 0.1 mg/kg/PO/72h, Metacam®) and antibiotics (8 mg/kg/SC, cefovecin, Convenia®, Zoetis, Louvain-La-Neuve, Belgium). The surgical sites and the teeth were disinfected three times a week using gauzes soaked in a chlorhexidine solution (0.12%, Perio-Aid Tratamiento®, Dentaid, Barcelona, Spain). Thereafter, a toothbrush with chlorhexidine gel (0.2%, Chlorhexidine Bioadhesive Gel, Lacer, Barcelona, Spain) was used three times weekly for plaque control. The animals received a soft-pellet diet for 1 week. The sutures were kept in place for 14 days.

The animals were sedated 8 weeks after the second phase by medetomidine (10 µg/kg/IM, Domitor®) and subsequently sacrificed with an overdose of sodium pentobarbital (60 mg/kg/IV, Dolethal®, Vetoquinol, France).

### 2.4 | Micro-CT

After euthanization, the maxilla and mandible of each animal were removed, and individual bone blocks containing the implanted

biomaterials and the surrounding soft and hard tissues were obtained and subsequently fixed in 10% buffered formalin.

The samples were scanned using a high-resolution micro-CT (SkyScan 1172, Bruker microCT NV, Kontig, Belgium). The X-ray source was set at 100Kv and 100  $\mu$ A with a pixel size of 13.54  $\mu$ m and the use of an aluminum/copper filter. Samples were scanned freshly placed in a gauze soaked in 10% buffered formalin and surrounded by a soft plastic sheet to avoid dehydration. Each sample was set on the object stage, and the scan was performed with a 360° rotation and images acquired every 0.4°. After scanning, images were reconstructed with a software (NRecon, Bruker microCT NV) based on the algorithm of Feldkamp<sup>37</sup> using the same parameters for all the samples (to allow comparison) and after the correction of the possible misalignment (smoothing=2; beam hardening=20; and ring artifact correction=4). Each defect was reconstructed separately. The reconstructed images were evaluated with a software (DataViewer, Bruker microCT NV) to place the defect in an anatomical position, setting in the same line the center of the mesial and distal roots. Later, the coronal and transaxial views were stored for analysis. The defect area was analyzed as the volume of interest (VOI) and highlighted using the apical and coronal notches as references. In each VOI, the % of bone substitute, new mineralized bone, total mineralized volume (bone substitute + new mineralized bone), and soft tissues were calculated.

## 2.5 | Histological procedures

After fixation, all 32 defect sites were dehydrated in an ascending series of ethanol and embedded in methyl methacrylate (MMA). After polymerization, the specimens were sectioned in a mesiodistal plane along the axis of the roots with a slow-speed diamond saw with a coolant (Varicut® VC-50; Leco, Munich, Germany). Thereafter, the approximately 600- $\mu$ m-thick ground sections were mounted on Plexiglas slabs and ground and polished (Knuth-Rotor-3; Struers, Rodovre/Copenhagen, Denmark) to a final thickness of 150  $\mu$ m. Finally, the sections were superficially stained with toluidine blue/McNeal combined with basic fuchsin. Photography was performed using a digital camera (AxioCam MRc; Carl Zeiss, Oberkochen, Germany) connected to a light microscope (Axio Imager M2; Carl Zeiss).

## 2.6 | Histometric analysis

The most central section (visible apical and coronal notches, presumably central position within the defect area) of each defect was chosen for histometric analysis. Regions of interest were digitalized with a computer connected to a light microscope. Thereafter, the following landmarks for histometric measurements (see below and Figure 2A) were identified and discussed by three investigators (L.C.W., J.-C.I., and D.D.B):

1. Gingival margin (GM)
2. Apical end of the junctional epithelium (aJE)
3. Apical end of the coronal notch (cN)
4. Highest point of new cementum (hNC)
5. Highest point of new bone (hNB)
6. Highest point of new continuous cementum new cementum without interruption (hCC)
7. Apical end of the apical notch (aN)

Since cementum formation was not always continuous from the apical notch to its most coronal extension, measurements were distinguished between the highest point of new cementum without interruption (new continuous cementum) and the highest point of cementum. The following vertical histometric measurements were performed along the axis running from the cemento-enamel junction to the apical root surface using a special software (Zeiss Efficient Navigation Pro, Carl Zeiss):

1. Defect height (aN - cN)
2. Junctional epithelium (JE) length + gingival sulcus depth (aJE - GM)
3. Connective tissue adhesion height (hNC - aJE)
4. Length from the apical notch to the highest point of new cementum (aN - hNC)
5. Length from the apical notch to the highest point of new continuous cementum (aN - hCC)
6. Height of new bone (aN - hNB)

The obtained absolute values for aN-hCC, aN-hNC, and aN-hNB were additionally calculated as relative values (i.e., in % of the defect height).

Additionally, to the vertical measurements, area measurements were performed to assess bone formation. To exclude the region where periodontal regeneration was measured (vertical distance measurements), the area measurements were confined to a region 0.5 mm away from the root surface. In this defect area, the area fractions (in %) of soft tissue, osteoid, new mineralized bone, bone substitutes, and total mineralized area (bone substitute + new mineralized bone) were calculated. Moreover, the % of new mineralized bone, osteoid, and soft tissue covering the surfaces of all bone substitute particles were calculated to assess the osteoconductivity.

## 2.7 | Statistical analysis

Since no comparable previous study and thus no data were available, a conclusive sample size calculation was not possible.

Data analyses were performed using a special software (Prism v7, GraphPad Software, La Jolla, CA, USA). All analyses were performed on animal level, and groups were compared using the Friedman test with Dunn's multiple comparisons testing. The Wilcoxon matched-pair signed-rank test with the Bonferroni-Holm correction was used when two groups were compared.



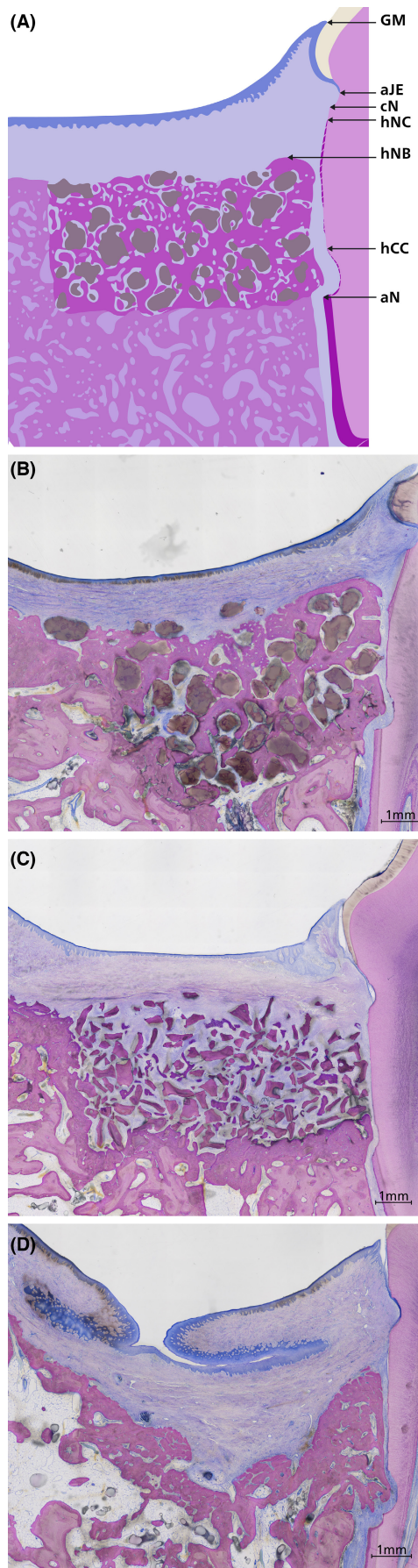


**FIGURE 2** (A) Histometric landmarks: aJE, apical end of junctional epithelium; aN, apical end of the apical notch; cN, apical end of the coronal notch; GM, gingival margin; hNB, highest point of new bone; hNC, highest point of new cementum; hCC, highest point of new continuous cementum. Representative overview of a histological section of (B) the test group, (C) the positive control group, and (D) the negative control group. Staining: toluidine blue/McNeal + basic fuchsin.

### 3 | RESULTS

#### 3.1 | Clinical findings

In total, 32 defects were created and filled with CO<sub>3</sub>Ap-BS (12 defects) and DBBM (12 defects) or left empty (8 defects). The healing was uneventful in all dogs without complications.

#### 3.2 | Descriptive histology

All 32 defects were available for descriptive analysis. Two to three ground sections per defect were evaluated. Heavy inflammatory signs (e.g., inflammatory infiltrate and mass of inflammatory cells) or pathological pocket formation were never observed. Representative histological overviews of all groups are presented in [Figure 2](#).

In all defects, new cementum, new bone, and new PDL were observed ([Figure 3](#)). However, the amount of new periodontal tissues varied from defect to defect. On a few root surfaces, remnants of superficially instrumented old cementum were observed. The cementum formation was at a very early stage, and in most cases, a very thin cementum layer was present. Moreover, the cementum formation from apical to coronal was mostly interrupted at a certain level and continued more coronally again.

Residual bone substitutes were seen in all defects of the test group and the positive control group ([Figure 4](#)). Signs of degradation (e.g., osteoclast-like cells and/or resorption pits) of the two biomaterials were very rarely observed ([Figure 4B,D](#)). The bone substitutes were never in direct contact with the root surface, and adverse events, such as ankylosis or root resorptions, were not detected. Moreover, away from the root surface, the bone substitutes were covered with new bone, osteoid, or soft tissue. In the test group treated with CO<sub>3</sub>Ap-BS, there was an obvious higher amount of new bone ([Figure 4A,B](#)) compared to the two control groups ([Figure 4C,D](#)). In the central part of all defects in control group 2, a lower vertical gain of bone height was observed, whereas the test group and the positive control group demonstrated more gain in bone height.

In more apical regions, the PDL appeared more mature, whereas more coronal regions showed less mature PDL. In addition, the collagen fibers of the newly formed PDL were occasionally perpendicularly inserted into the newly formed cementum but in most cases fiber insertion was not visible.



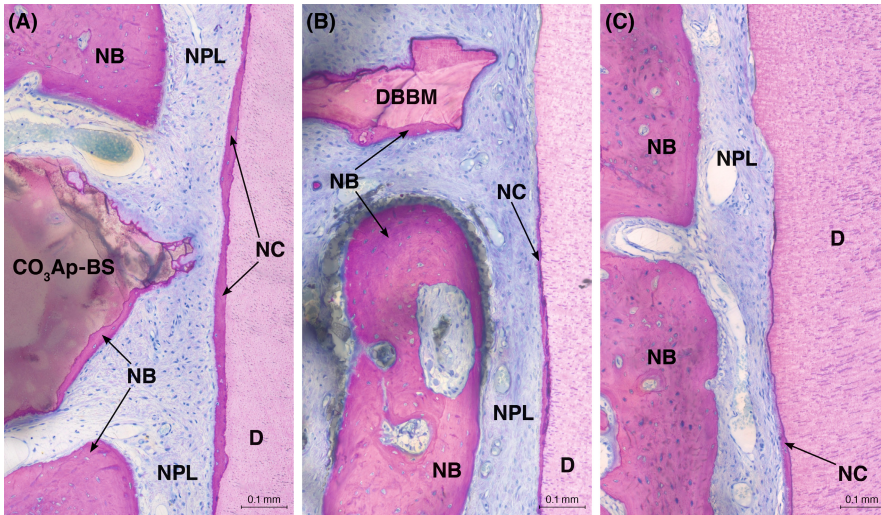


**FIGURE 3** Periodontal regeneration in (A) the test group, (B) the positive control group, and (C) the negative control group. Staining: toluidine blue/McNeal + basic fuchsin. CO<sub>3</sub>Ap-BS, carbonate apatite bone substitute; D, dentin; DBBM, deproteinized bovine bone mineral; NB, new bone; NC, new cementum; NPL, new periodontal ligament.

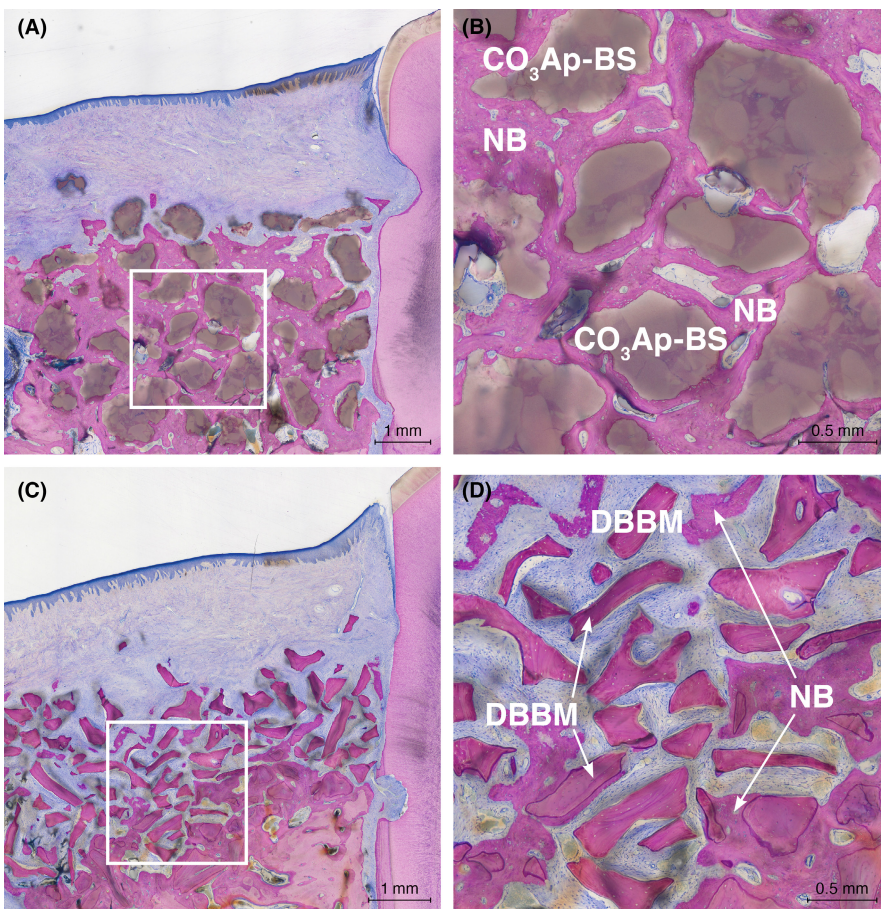


**FIGURE 4** Overview of a histological section showing the osseointegration of the biomaterial in (A) the test group and (C) the positive control group. The yellow squares are showing an area of higher magnification for (B) the test group (D) and the positive control group. Staining: toluidine blue/McNeal + basic fuchsin. CO<sub>3</sub>Ap-BS, carbonate apatite bone substitute; DBBM, deproteinized bovine bone mineral; NB, new bone.

### 3.3 | Histometry and micro-CT

#### 3.3.1 | Distance measurements

Out of 32 defects, one defect of the test group was not available for histometric analysis because of a misangulated cutting direction. Therefore, 11 defects of the test group, 12 defects of the positive control group, and 8 defects of the negative control group were suitable for histometry. The histometric measurements are presented in [Figure 5A](#) (full dataset is presented in [Table S1](#)). No statistically

significant differences were observed between the test and control groups for defect height. The mean value for the JE including the sulcus depth was higher in the test group and the positive control group compared to the negative control group without statistical significance ( $p = .471$  and  $p = .231$ , respectively). The values for the highest point of new continuous cementum and the highest point of new cementum were similar and did not reach statistical significance ( $p > .999$ ). Furthermore, absolute and relative values for new bone formation along the tooth root were statistically not different between all three groups.

### 3.3.2 | Area and volumetric measurements

The area fraction analysis (Figure 5B; full data are presented in Table S2) on the histological sections demonstrated statistically significantly fewer soft tissues in the bony defect of the test group ( $28.07 \pm 8.41\%$ ), as compared to the negative control group ( $58.76 \pm 6.89\%$ ,  $p = .014$ ). New mineralized bone area was statistically significantly higher in the defects of the test group ( $38.46 \pm 5.37\%$ ) compared to the positive control group ( $21.05 \pm 5.50\%$ ,  $p = .040$ ). The total mineralized area was statistically significantly higher in the test group ( $66.06 \pm 9.34\%$ ) compared to the negative control group ( $36.11 \pm 6.40\%$ ,  $p = .014$ ).

The data of the micro-CT analysis are demonstrated in Figure 5C (full data are available in Table S3). Representative radiographs of the three groups are presented in Figure 6. Regarding the % of soft tissue within the defect volume, a statistically significant difference was found comparing the test group ( $30.26 \pm 2.95\%$ ) with the negative control group ( $57.32 \pm 8.63\%$ ,  $p = .014$ ). The total mineralized volume (new mineralized bone + biomaterial) was statistically significantly higher in favor of the test group ( $69.74 \pm 2.95\%$ ) compared to the negative control group ( $42.68 \pm 8.68\%$ ,  $p = .014$ ) but not to the positive control group ( $52.94 \pm 3.63\%$ ,  $>0.999$ ).

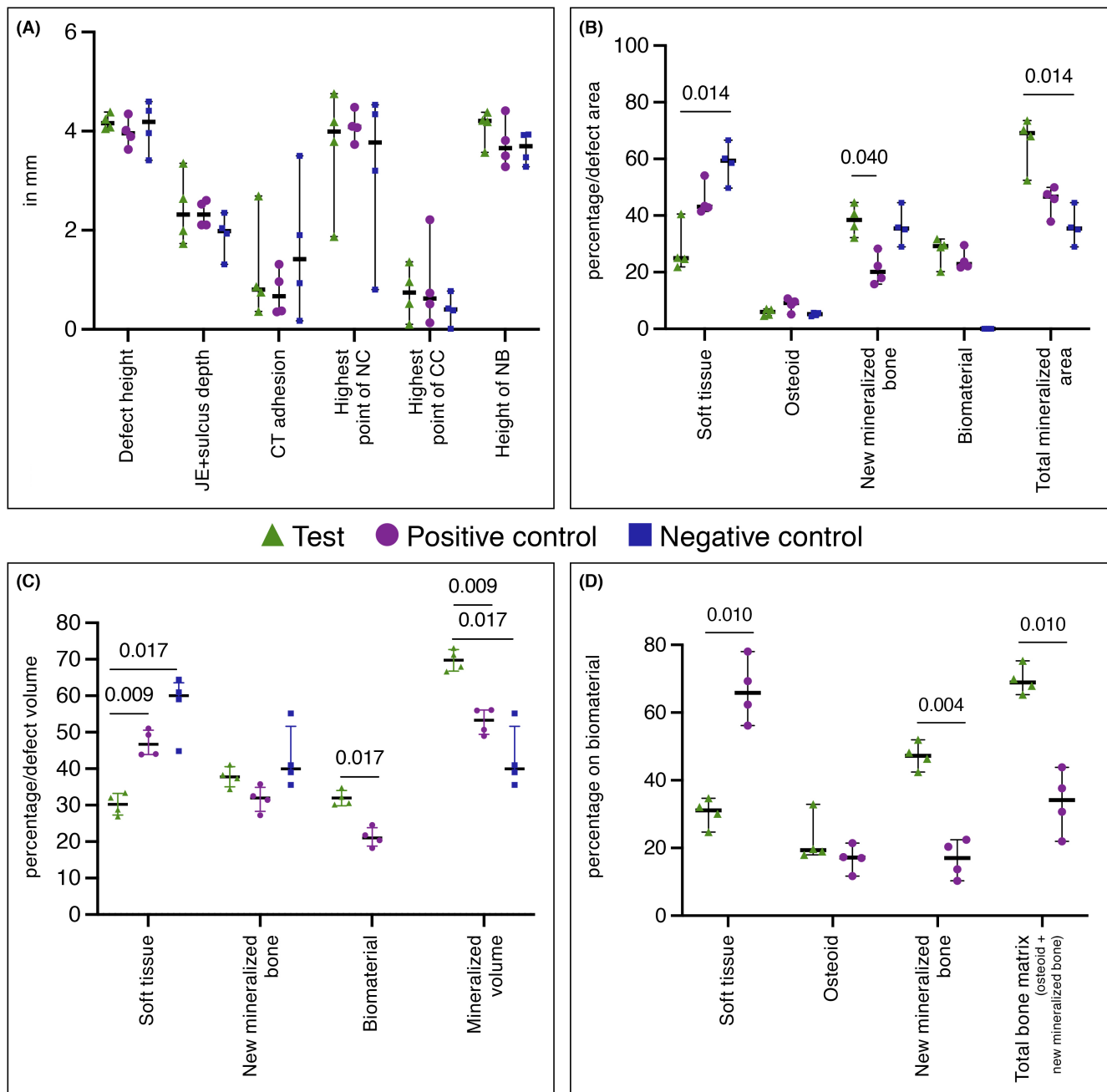


FIGURE 5 Graphical illustrations of (A) histometric measurements, (B) area measurements on histological sections, (C) volumetric measurements on micro-CT, and (D) osteoconductivity analysis. Statistical significance was set at .05.

### 3.3.3 | Osteoconductivity

The osteoconductive analysis (Figure 5D) revealed a faster osseointegration of the CO<sub>3</sub>Ap-BS granules as demonstrated more bone matrix (new mineralized bone + osteoid) on the surfaces of the bone substitute particles compared to the positive control group (69.59 ± 4.23% vs. 33.53 ± 9.38%, *p* = .114). Consequently, there was less soft tissue on the particles of the test group compared to the positive control group (30.41 ± 4.23% vs. 66.48 ± 9.38%, *p* = .114). Furthermore, the value for osteoid on the grafted particles in the test group (22.38 ± 7.03%) was higher compared to the positive control group (16.84 ± 3.98%, *p* = .800). All the data regarding osteoconductivity are presented in Table S4.

## 4 | DISCUSSION

The present study has investigated the potential of a novel synthetic bone substitute (CO<sub>3</sub>Ap-BS) on the healing of acute-type three-wall intrabony defects in dogs. To the best of our knowledge, this is the first histological study which has evaluated this biomaterial in regenerative periodontal therapy. Compared to DBBM, which is one of the best-documented biomaterials used for periodontal and bone reconstructive procedures, the present findings revealed very promising effects of CO<sub>3</sub>Ap-BS on periodontal regeneration evidenced by formation of cementum, bone, and PDL. The CO<sub>3</sub>Ap-BS showed excellent biocompatibility as demonstrated by extensive osseointegration and absence of inflammation. A very interesting finding was the increased bone formation and higher osteoconductivity obtained with CO<sub>3</sub>Ap-BS as compared to DBBM.

Nowadays, periodontal reconstructive/regenerative surgeries are performed with different biomaterials, including bone substitutes.<sup>9</sup> Some of these biomaterials result histologically in periodontal regeneration and improved clinical outcomes evidenced by pocket depth reduction, clinical attachment level gain, and hard tissue fill in intrabony and furcation defects.<sup>7-9,38</sup> DBBM is one of the best-documented materials in periodontal reconstructive surgery. This material has shown to promote periodontal regeneration in intrabony defects as demonstrated in animal and human histological studies.<sup>14,15,39</sup> In contrast, as of today, histological evidence substantiating the ability of alloplastic materials to facilitate periodontal regeneration remains primarily confined to animal models. In humans, the healing process has predominantly exhibited a reparative nature, distinguished by the development of a long junctional epithelium and the encapsulation of graft particles by connective tissue. Limited periodontal regeneration has been observed primarily at the apical region of the defects.<sup>9</sup> A systematic review of periodontal regeneration in animal models revealed that cementum regeneration amounted to 33%–75% and bone regeneration to 12%–75% of the original defect depth with various biomaterials.<sup>40</sup> Xenografts alone demonstrated 47% new cementum and 27% new bone formation, whereas alloplastic materials alone have shown 61% new cementum

and 56% new bone formation. The present study showed in the defects treated with DBBM 22.47% new continuous cementum and 103.20% when the highest point of cementum was measured. In the defects treated with CO<sub>3</sub>Ap-BS, the length of the new continuous cementum measured 17.54% and 99.59% if the highest point of cementum was analyzed. The new bone height measured 94.22% in the group treated with DBBM and 97.92% following grafting with CO<sub>3</sub>Ap-BS. However, it is important to point out that it is very difficult to compare the cementum formation measured in the present study with the values reported previously since, until now, only our group has published data about continuous cementum and the highest point of cementum.<sup>36</sup> It may thus be speculated that other groups have just reported the highest point of the cementum formation without taking the discontinuity into account. Nevertheless, it remains a possibility that the elevated levels of bone formation observed in this study could, to some extent, be influenced by the configuration of the defect (specifically, a contained bony defect) known for its pronounced self-healing potential.

Many effects such as cell response, angiogenesis, and bone formation are influenced by the architecture and surface properties of a bone substitute.<sup>41</sup> The most important parameters include surface and physical properties such as pore size, shape, and porosity.<sup>41,42</sup> Both DBBM and CO<sub>3</sub>Ap-BS are carbonate apatite with low crystallinity as shown by X-ray diffraction and Fourier transform infrared.<sup>28</sup> CO<sub>3</sub>Ap-BS showed a higher content of carbonate apatite and a higher crystallinity, but a lower porosity compared to DBBM.<sup>28</sup> Usually, a higher porosity and lower crystallinity is leading to an improved cell viability, migration, and proliferation.<sup>41</sup> Nevertheless, the biomaterial with less porosity and a higher crystallinity (i.e., CO<sub>3</sub>Ap-BS) showed an accelerated bone formation in this study. As suggested by Fujisawa et al.,<sup>28</sup> the higher content of carbonate in CO<sub>3</sub>Ap-BS compared to DBBM may be the reason for faster bone formation. Carbonate has shown to be a determining factor for the osteoconductivity of apatites.<sup>43</sup> The higher the carbonate content in a biomaterial, the higher the osteoclastic resorption at the biomaterial's surface.<sup>44</sup> Osteoclasts release chemokines which are activating osteoblasts by cell-to-cell interactions.<sup>43</sup> Moreover, a higher content of carbonate promoted cell proliferation of murine preosteoblasts and enhanced the calcium release.<sup>34</sup> Thus, all aforementioned properties of CO<sub>3</sub>Ap-BS may have contributed to the enhanced bone formation compared to the group treated with DBBM.

It has been demonstrated that the degradation rate of DBBM is very slow.<sup>45</sup> However, in the present study, no differences in terms of resorption of the used biomaterials were detected. The faster degradation rate of the CO<sub>3</sub>Ap-BS compared to DBBM was shown in an animal model and was attributed to the higher content of carbonate.<sup>28</sup>

One limitation of the present study is the fact that it was performed in an animal model which may not adequately reflect the clinical scenario. Nevertheless, the dog model is still one of the best-established animal models in periodontal research.<sup>46,47</sup> Translation of the results to the human situation may still be challenging due to inherent differences in anatomy and physiology.



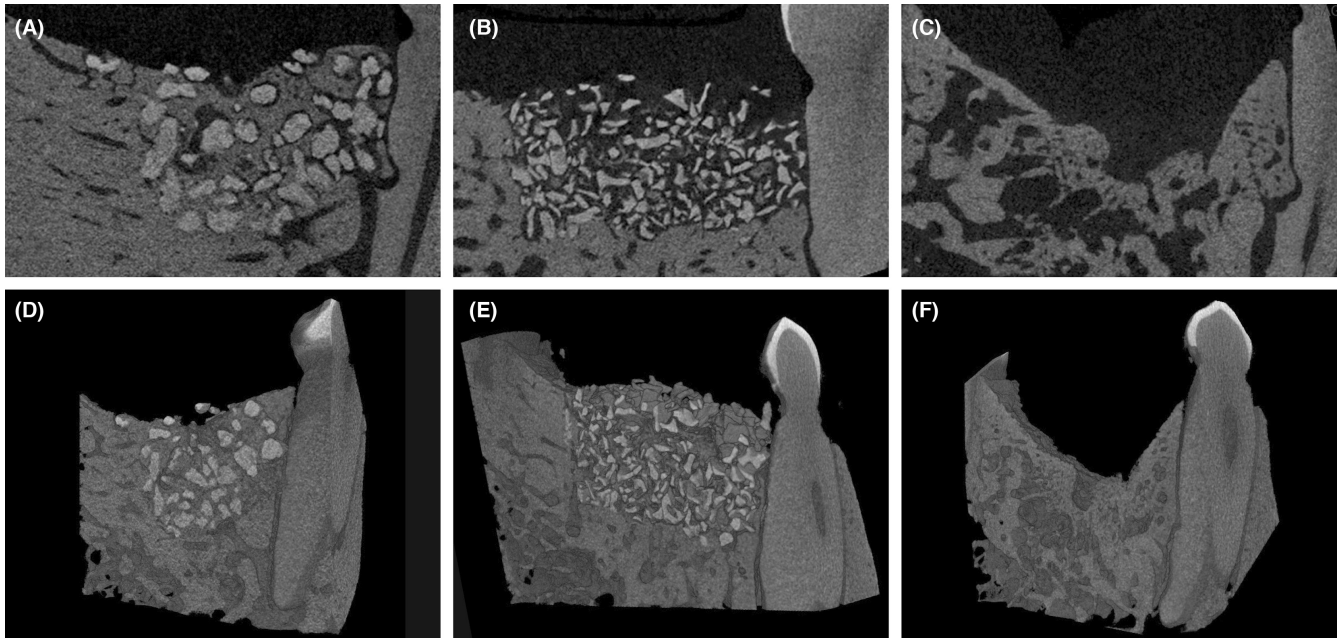


**FIGURE 6** Representative micro-CT images of (A) the test group, (B) the positive control group, and (C) the negative control group.

Furthermore, it is well known that acute-type defects and chronic periodontal defects may not have the same morphology. In addition, the bacterial challenge and immunoreaction are much more pronounced in chronic defects.<sup>48,49</sup> Moreover, the spontaneous healing potential is higher in acute-type defects compared to chronic ones.<sup>50,51</sup> However, there is evidence demonstrating that the potential for periodontal regeneration is similar on planed root surfaces previously exposed to periodontal disease to that of acute-type defects where the root surfaces were surgically deprived of their attachment apparatus.<sup>47</sup> Therefore, despite these limitations, the used animal model is well accepted for studies on periodontal regeneration having also the advantages of creating standardized defects.<sup>48,49</sup> Finally, it has to be taken into account that the statistical analyses were set on animal level with a sample size of only 4.

Since, according to the best of our knowledge, this was the first study evaluating this  $\text{CO}_3\text{Ap-BS}$  for periodontal regeneration, only one timepoint was investigated, and therefore, no evaluation of early healing events and the sequence of healing was possible. Obviously, evaluation of the resorption process of the biomaterials would only be possible by using different healing periods.

The positive findings regarding the osteoconductivity and bone formation with the use of  $\text{CO}_3\text{Ap-BS}$  are in line with the results reported in other preclinical studies.<sup>28,32,35,43</sup> Mano et al.<sup>43</sup> investigated the osteoconductivity of three apatitic bone substitutes with different carbonate contents in combination with simultaneous installation of dental implants in an animal model. They observed that the bone-to-implant contact ratio and the area of new bone were larger with the use of  $\text{CO}_3\text{Ap-BS}$  compared to DBBM. Additionally, they observed a better preservation of the alveolar ridge with  $\text{CO}_3\text{Ap-BS}$ . The same observation was made in the present study, with a good preserved alveolar ridge away from

the tooth surface and the largest area of new bone as shown by micro-CT and histometry in the test group. Interestingly, Egashira et al.<sup>52</sup> very recently showed a faster soft tissue healing after tooth extraction with the use of  $\text{CO}_3\text{Ap-BS}$  as compared to empty sockets and a hydroxyapatite bone substitute. Additionally, they found in an *in vitro* analysis a high collagen expression by fibroblasts and a downregulation of the activity of oral epithelial cells on carbonate apatite. This may be beneficial if it comes to periodontal regeneration since the migration of epithelial cells should be avoided to give the PDL cells enough time to establish a provisional matrix for a new attachment apparatus. Very recently, a clinical study has evaluated the potential of  $\text{CO}_3\text{Ap-BS}$  in combination with FGF-2 in a single-arm clinical trial.<sup>29</sup> The results revealed good clinical improvements in terms of clinical attachment level gain, probing depth reduction, and bleeding on probing reduction without any adverse events, which is in line with the clinical observations made in the present study.

The results of the present study open a wide field for future investigations on the potential use of this new synthetic bone substitute. An inherent question is whether a combination of  $\text{CO}_3\text{Ap-BS}$  with growth and differentiation factors may additionally enhance periodontal regeneration compared to the use of  $\text{CO}_3\text{Ap-BS}$  alone. Furthermore, it is unknown to what extent  $\text{CO}_3\text{Ap-BS}$  may enhance periodontal wound healing/regeneration in furcation defects. Finally,  $\text{CO}_3\text{Ap-BS}$  should be also evaluated in human randomized clinical trials in intrabony and furcation defects.

## 5 | CONCLUSION

Taken together, the present results have for the first time provided histological evidence for the potential of this novel synthetic bone



substitute to facilitate periodontal and bone regeneration, thus warranting further preclinical and clinical testing.

## ACKNOWLEDGEMENTS

The authors express their special thanks to the staff at the Veterinary Faculty Lugo, University of Santiago de Compostela, Spain, for excellent handling of the animals, to Silvia Owusu (laboratory technicians, Robert K. Schenk Laboratory of Oral Histology at the School of Dental Medicine, University of Bern) for the extensive help during histological processing, and to Bernadette Rawyler and Ines Badertscher for the professional illustrations. Moreover, the authors would like to thank GC Corporation for the financial support. The primary investigator (J.-C. I.) would like to thank the Osteology Foundation for a one-year Scholarship in 2021.

## FUNDING INFORMATION

This study was financially supported by a grant from GC Corporation.

## CONFLICT OF INTEREST STATEMENT

This study was financially supported by a grant from GC Corporation. Dr. Imber received an Osteology Research Scholarship in 2021. Dr. Rocuzzo is the recipient of an ITI Scholarship in 2022. All the authors report to have no other potential conflict of interest related to this article.

## DATA AVAILABILITY STATEMENT

The data that support the findings of this study are available in the supplementary material of this article. If additional data are needed, they are available from the corresponding author upon reasonable request.

## ORCID

Jean-Claude Imber  <https://orcid.org/0000-0001-6690-5249>

Andrea Rocuzzo  <https://orcid.org/0000-0002-8079-0860>

Alexandra Stähli  <https://orcid.org/0000-0002-5631-3300>

Fernando Muñoz  <https://orcid.org/0000-0002-4130-1526>

Jens Weusmann  <https://orcid.org/0000-0002-4323-5040>

Dieter Daniel Bosshardt  <https://orcid.org/0000-0002-2132-6363>

Anton Sculean  <https://orcid.org/0000-0003-2836-5477>

## REFERENCES

- Darveau RP, Curtis MA. Oral biofilms revisited: a novel host tissue of bacteriological origin. *Periodontol 2000*. 2021;86(1):8-13.
- Jakubovics NS, Goodman SD, Mashburn-Warren L, Stafford GP, Cieplik F. The dental plaque biofilm matrix. *Periodontol 2000*. 2021;86(1):32-56.
- Joseph S, Curtis MA. Microbial transitions from health to disease. *Periodontol 2000*. 2021;86(1):201-209.
- Sanz M, Herrera D, Kecsull M, et al. Treatment of stage I-III periodontitis—the EFP S3 level clinical practice guideline. *J Clin Periodontol*. 2020;47(S22):4-60.
- Matuliene G, Pjetursson BE, Salvi GE, et al. Influence of residual pockets on progression of periodontitis and tooth loss: results after 11 years of maintenance. *J Clin Periodontol*. 2008;35(8):685-695.
- Reynolds MA, Kao RT, Camargo PM, et al. Periodontal regeneration – intrabony defects: a consensus report from the AAP Regeneration Workshop. *J Periodontol*. 2015;86(2 Suppl):S105-S107.
- Kao RT, Nares S, Reynolds MA. Periodontal regeneration – intrabony defects: a systematic review from the AAP Regeneration Workshop. *J Periodontol*. 2015;86(2 Suppl):S77-S104.
- Nibali L, Koidou VP, Nieri M, Barbato L, Pagliaro U, Cairo F. Regenerative surgery versus access flap for the treatment of intra-bony periodontal defects: a systematic review and meta-analysis. *J Clin Periodontol*. 2020;47(Suppl 22):320-351.
- Sculean A, Nikolidakis D, Nikou G, Ivanovic A, Chapple IL, Stavropoulos A. Biomaterials for promoting periodontal regeneration in human intrabony defects: a systematic review. *Periodontol 2000*. 2015;68(1):182-216.
- Froum SJ, Kushner L, Stahl SS. Healing responses of human intraosseous lesions following the use of debridement, grafting and citric acid root treatment. I. Clinical and histologic observations six months postsurgery. *J Periodontol*. 1983;54(2):67-76.
- Nabers CL, Reed OM, Hamner JE 3rd. Gross and histologic evaluation of an autogenous bone graft 57 months postoperatively. *J Periodontol*. 1972;43(11):702-704.
- Bowers GM, Chadroff B, Carnevale R, et al. Histologic evaluation of new attachment apparatus formation in humans. Part I. *J Periodontol*. 1989;60(12):664-674.
- Koylass JM, Valderrama P, Mellonig JT. Histologic evaluation of an allogeneic mineralized bone matrix in the treatment of periodontal osseous defects. *Int J Periodontics Restorative Dent*. 2012;32(4):405-411.
- Camelo M, Nevins ML, Schenk RK, et al. Clinical, radiographic, and histologic evaluation of human periodontal defects treated with Bio-Oss and Bio-Gide. *Int J Periodontics Restorative Dent*. 1998;18(4):321-331.
- Sculean A, Windisch P, Keglevich T, Chiantella GC, Gera I, Donos N. Clinical and histologic evaluation of human intrabony defects treated with an enamel matrix protein derivative combined with a bovine-derived xenograft. *Int J Periodontics Restorative Dent*. 2003;23(1):47-55.
- Nyman S, Lindhe J, Karring T, Rylander H. New attachment following surgical treatment of human periodontal disease. *J Clin Periodontol*. 1982;9(4):290-296.
- Sculean A, Donos N, Chiantella GC, Windisch P, Reich E, Brex M. GTR with bioresorbable membranes in the treatment of intrabony defects: a clinical and histologic study. *Int J Periodontics Restorative Dent*. 1999;19(5):501-509.
- Heijl L. Periodontal regeneration with enamel matrix derivative in one human experimental defect. A case report. *J Clin Periodontol*. 1997;24(9 Pt 2):693-696.
- Sculean A, Donos N, Windisch P, et al. Healing of human intrabony defects following treatment with enamel matrix proteins or guided tissue regeneration. *J Periodontol Res*. 1999;34(6):310-322.
- Froum S, Stahl SS. Human intraosseous healing responses to the placement of tricalcium phosphate ceramic implants. II. 13 to 18 months. *J Periodontol*. 1987;58(2):103-109.
- Horváth A, Stavropoulos A, Windisch P, Lukács L, Gera I, Sculean A. Histological evaluation of human intrabony periodontal defects treated with an unsintered nanocrystalline hydroxyapatite paste. *Clin Oral Investig*. 2013;17(2):423-430.
- Sculean A, Windisch P, Keglevich T, Gera I. Clinical and histologic evaluation of an enamel matrix protein derivative combined with a bioactive glass for the treatment of intrabony periodontal defects in humans. *Int J Periodontics Restorative Dent*. 2005;25(2):139-147.
- Stahl SS, Froum SJ. Histologic and clinical responses to porous hydroxylapatite implants in human periodontal defects. Three to twelve months postimplantation. *J Periodontol*. 1987;58(10):689-695.

24. Miron RJ, Gruber R, Hedbom E, et al. Impact of bone harvesting techniques on cell viability and the release of growth factors of autografts. *Clin Implant Dent Relat Res*. 2013;15(4):481-489.
25. Miron RJ, Hedbom E, Saulacic N, et al. Osteogenic potential of autogenous bone grafts harvested with four different surgical techniques. *J Dent Res*. 2011;90(12):1428-1433.
26. Bouler JM, Pilet P, Gauthier O, Verron E. Biphasic calcium phosphate ceramics for bone reconstruction: a review of biological response. *Acta Biomater*. 2017;53:1-12.
27. Jin P, Liu L, Cheng L, Chen X, Xi S, Jiang T. Calcium-to-phosphorus releasing ratio affects osteoinductivity and osteoconductivity of calcium phosphate bioceramics in bone tissue engineering. *Biomed Eng*. 2023;22(1):12.
28. Fujisawa K, Akita K, Fukuda N, et al. Compositional and histological comparison of carbonate apatite fabricated by dissolution-precipitation reaction and Bio-Oss®. *J Mater Sci Mater Med*. 2018;29(8):121.
29. Kitamura M, Yamashita M, Miki K, et al. An exploratory clinical trial to evaluate the safety and efficacy of combination therapy of REGROTH® and Cytrans® granules for severe periodontitis with intrabony defects. *Regen Ther*. 2022;21:104-113.
30. Kudoh K, Fukuda N, Kasugai S, et al. Maxillary sinus floor augmentation using low-crystalline carbonate apatite granules with simultaneous implant installation: first-in-human clinical trial. *J Oral Maxillofac Surg*. 2019;77(5):985.e1-985.e11.
31. Nagata K, Fuchigami K, Kitami R, et al. Comparison of the performances of low-crystalline carbonate apatite and Bio-Oss in sinus augmentation using three-dimensional image analysis. *Int J Implant Dent*. 2021;7(1):24.
32. Sato N, Handa K, Venkataiah VS, et al. Comparison of the vertical bone defect healing abilities of carbonate apatite,  $\beta$ -tricalcium phosphate, hydroxyapatite and bovine-derived heterogeneous bone. *Dent Mater J*. 2020;39(2):309-318.
33. Hayashi K, Kishida R, Tsuchiya A, Ishikawa K. Honeycomb blocks composed of carbonate apatite,  $\beta$ -tricalcium phosphate, and hydroxyapatite for bone regeneration: effects of composition on biological responses. *Mater Today Bio*. 2019;4:100031.
34. Fujioka-Kobayashi M, Tsuru K, Nagai H, et al. Fabrication and evaluation of carbonate apatite-coated calcium carbonate bone substitutes for bone tissue engineering. *J Tissue Eng Regen Med*. 2018;12(10):2077-2087.
35. Ishikawa K, Miyamoto Y, Tsuchiya A, Hayashi K, Tsuru K, Ohe G. Physical and histological comparison of hydroxyapatite, carbonate apatite, and  $\beta$ -tricalcium phosphate bone substitutes. *Materials (Basel)*. 2018;11(10):2077-2087.
36. Imber JC, Bosshardt DD, Stähli A, Saulacic N, Deschner J, Sculean A. Preclinical evaluation of the effect of a volume-stable collagen matrix on periodontal regeneration in two-wall intrabony defects. *J Clin Periodontol*. 2021;48:560-569.
37. Feldkamp LA, Davis LC, Kress JW. Practical cone-beam algorithm. *J Opt Soc Am A*. 1984;1(6):612-619.
38. Jepsen S, Gennai S, Hirschfeld J, Kalemaj Z, Buti J, Graziani F. Regenerative surgical treatment of furcation defects: a systematic review and Bayesian network meta-analysis of randomized clinical trials. *J Clin Periodontol*. 2020;47(Suppl 22):352-374.
39. Ivanovic A, Bosshardt DD, Mihatic I, Schwarz F, Gruber R, Sculean A. Effect of pulverized natural bone mineral on regeneration of three-wall intrabony defects. A preclinical study. *Clin Oral Invest*. 2014;18(4):1319-1328.
40. Ivanovic A, Nikou G, Miron RJ, Nikolidakis D, Sculean A. Which biomaterials may promote periodontal regeneration in intrabony periodontal defects? A systematic review of preclinical studies. *Quintessence Int*. 2014;45(5):385-395.
41. Bobbert FSL, Zadpoor AA. Effects of bone substitute architecture and surface properties on cell response, angiogenesis, and structure of new bone. *J Mater Chem B*. 2017;5(31):6175-6192.
42. Davison NL, ten Harkel B, Schoenmaker T, et al. Osteoclast resorption of beta-tricalcium phosphate controlled by surface architecture. *Biomaterials*. 2014;35(26):7441-7451.
43. Mano T, Akita K, Fukuda N, et al. Histological comparison of three apatitic bone substitutes with different carbonate contents in alveolar bone defects in a beagle mandible with simultaneous implant installation. *J Biomed Mater Res B Appl Biomater*. 2020;108(4):1450-1459.
44. Deguchi K, Nomura S, Tsuchiya A, Takahashi I, Ishikawa K. Effects of the carbonate content in carbonate apatite on bone replacement. *J Tissue Eng Regen Med*. 2022;16(2):200-206.
45. Jensen SS, Brogini N, Hjörting-Hansen E, Schenk R, Buser D. Bone healing and graft resorption of autograft, anorganic bovine bone and  $\beta$ -tricalcium phosphate. A histologic and histomorphometric study in the mandibles of minipigs. *Clin Oral Implants Res*. 2006;17(3):237-243.
46. Kantarci A, Hasturk H, Van Dyke TE. Animal models for periodontal regeneration and peri-implant responses. *Periodontol 2000*. 2015;68(1):66-82.
47. Struillou X, Boutigny H, Soueidan A, Layrolle P. Experimental animal models in periodontology: a review. *Open Dent J*. 2010;4:37-47.
48. Donos N, Park JC, Vajgel A, de Carvalho FB, Dereka X. Description of the periodontal pocket in preclinical models: limitations and considerations. *Periodontol 2000*. 2018;76(1):16-34.
49. Selvig KA. Discussion: animal models in reconstructive therapy. *J Periodontol*. 1994;65(12):1169-1172.
50. Lee JS, Wikesjö UM, Jung UW, et al. Periodontal wound healing/regeneration following implantation of recombinant human growth/differentiation factor-5 in a beta-tricalcium phosphate carrier into one-wall intrabony defects in dogs. *J Clin Periodontol*. 2010;37(4):382-389.
51. Park JC, Wikesjö UM, Koo KT, et al. Maturation of alveolar bone following implantation of an rhGDF-5/PLGA composite into 1-wall intra-bony defects in dogs: 24-week histometric observations. *J Clin Periodontol*. 2012;39(6):565-573.
52. Egashira Y, Atsuta I, Narimatsu I, et al. Effect of carbonate apatite as a bone substitute on oral mucosal healing in a rat extraction socket: in vitro and in vivo analyses using carbonate apatite. *Int J Implant Dent*. 2022;8(1):11.

## SUPPORTING INFORMATION

Additional supporting information can be found online in the Supporting Information section at the end of this article.

**How to cite this article:** Imber J-C, Imber LC, Rocuzzo A, et al. Preclinical evaluation of a new synthetic carbonate apatite bone substitute on periodontal regeneration in intrabony defects. *J Periodont Res*. 2023;00:1-11. doi:[10.1111/jre.13203](https://doi.org/10.1111/jre.13203)